Oncogene (2012), 1–12

www.nature.com/onc

ORIGINAL ARTICLE

RhoD participates in the regulation of cell-cycle progression and centrosome duplication

A Kyrkou[1,2], M Soufi[1], R Bahtz[3], C Ferguson[4], M Bai[5], RG Parton[4], I Hoffmann[3], M Zerial[6], T Fotsis[1,2] and C Murphy[2]

We have previously identified a Rho protein, RhoD, which localizes to the plasma membrane and the early endocytic compartment. Here, we show that a GTPase-deficient mutant of RhoD, RhoDG26V, causes hyperplasia and perturbed differentiation of the epidermis, when targeted to the skin of transgenic mice. *In vitro*, gain-of-function and loss-of-function approaches revealed that RhoD is involved in the regulation of G1/S-phase progression and causes overduplication of centrosomes. Centriole overduplication assays in aphidicolin-arrested p53-deficient U2OS cells, in which the cell and the centrosome cycles are uncoupled, revealed that the effects of RhoD and its mutants on centrosome duplication and cell cycle are independent. Enhancement of G1/S-phase progression was mediated via Diaph1, a novel effector of RhoD, which we have identified using a two-hybrid screen. These results indicate that RhoD participates in the regulation of cell-cycle progression and centrosome duplication.

Oncogene advance online publication, 4 June 2012; doi:10.1038/onc.2012.195

Keywords: RhoD; proliferation; centrosome cycle

INTRODUCTION

The human Rho family of small GTPases represents a major branch of the Ras superfamily, which participates in the regulation of various processes such as the formation of cellular protrusions, vesicular trafficking, transcriptional regulation, cell motility and cell cycle reviewed in Jaffe and Hall.[1] Rho GTPases exert their cytoskeletal actions mainly via the Diaphanous-Related Formins, the Wiskott–Aldrich syndrome protein and Wiskott–Aldrich syndrome protein-family verprolin-homologous proteins, reviewed in Sit and Manser.[2] The Diaphanous-Related Formin family comprising three paralog genes: Diaphanous 1, 2 and 3. Human Diaph1 is homologous to murine mDia1 with a 91% protein identity, whereas Diaph2 is homologous to mDia3, and Diaph3 to mDia2. The best-studied member of this family is Diaph1/mDia1, which has been implicated in a variety of processes from cytoskeletal rearrangements[3–6] to the regulation of the cell-cycle progression.[7,8]

The aberrant function of Ras and Rho GTPases contributes differentially to the development of cancer.[9,10] In contrast to Ras, where a plethora of mutations is found in ~30% of human cancers, in the case of Rho GTPases the mechanisms involve alterations in the expression and activation levels.[10] Mutations of Rho proteins in cancer have not been found to date, the only rearrangement reported is that of the *RhoH* gene found in non-Hodgkin's lymphoma and multiple myeloma.[11] Also, a splice variant of Rac1 (Rab1b) has been implicated in transformation.[12,13] Thus, characterizing the contribution of a Rho family member to cancer or generally cell proliferation requires an understanding of how its activity is regulated in normal and cancerous cells.

We have previously identified a Rho GTPase, RhoD and shown that it is localized on early endosomes, through which it alters membrane dynamics in the endocytic pathway[14] and inhibits the motility of endothelial[15] and 10T1/2 cells.[16] Moreover, RhoD induces the disassembly of stress fibres and focal adhesions,[14] and seems to antagonize the effect of RhoA at least on stress fibre formation.[16] Furthermore, RhoDG26V induced multinucleation and defective cytokinesis.[16] The known effectors of RhoD are HDia2C,[17] Plexin-A1[18] and Plexin-B1.[19] Even though it seems that RhoD provides a molecular link between the cytoskeleton and membrane trafficking, the mechanisms and molecules integrating these interactions at the level of cell proliferation are unclear. Motivated by the above-mentioned *in-vitro* effects, we addressed in the present study the role of RhoD *in vivo*. Driving the expression of RhoDG26V to the skin of transgenic mice, we observed increased cell proliferation and alterations in epidermal differentiation. *In-vitro* experiments demonstrated that RhoD enhances G1/S-phase progression via interaction with a novel effector, Diaphanous1/Diaph1 and causes overduplication of centrosomes in a G1/S progression-independent manner.

RESULTS

RhoDG26V expression causes hyperplasia accompanied by altered differentiation throughout the epidermis of transgenic mice

We generated transgenic mice expressing the GTPase-deficient mutant of RhoD, RhoDG26V, using the well-characterized K14 promoter to drive transgene expression to the basal layer of the epidermis. The transgenic mice exhibited three phenotypic characteristics: (1) a severe phenotype in the tail and ear

[1]Laboratory of Biological Chemistry, University of Ioannina Medical School, Ioannina, Greece; [2]Department of Biomedical Research, Foundation for Research and Technology-Hellas, Institute of Molecular Biology and Biotechnology, University Campus of Ioannina, Ioannina, Greece; [3]Cell Cycle Control and Carcinogenesis, German Cancer Research Center (DKFZ), Heidelberg, Germany; [4]Institute for Molecular Bioscience and Centre for Microscopy and Microanalysis, The University of Queensland, Brisbane, Queensland, Australia; [5]Department of Pathology, University of Ioannina Medical School, Ioannina, Greece and [6]Max Planck Institute for Molecular Cell Biology and Genetics, Dresden, Germany. Correspondence: Dr C Murphy, Department of Biomedical Research, Foundation for Research and Technology-Hellas, Institute of Molecular Biology and Biotechnology, University Campus of Ioannina, 45110 Ioannina, Greece.
E-mail: cmurphy@cc.uoi.gr
Received 26 September 2011; revised 12 April 2012; accepted 15 April 2012

characterized by discoloration, edema and skin detachment, (2) the animals often had flaky skin on the paw and digits, and (3) as the animals aged many lose body hair and have open wounds aggravated by constant scratching. In the case of the tail, the phenotype progresses until finally the mice lose the tail completely. No such phenotypes were seen in non-transgenic littermates.

Histopathological examination revealed hyperplasia in all layers of the epidermis and the epithelial cells of the hair follicles of the body skin (Figure 1b) and the ears of the transgenic mice (Figure 1d), while no such alterations were found in non-transgenic littermate controls (Figures 1a and c, respectively). In agreement, BrdU-labeled cells were increased in the basal layer (Supplementary Figure 1b) compared with non-transgenic littermates (Supplementary Figure 1a), being also readily detected in the suprabasal layers (Supplementary Figure 1c). Likewise, PCNA (proliferating cell nuclear antigen)-positive cells were found in the suprabasal layers of the transgenic mice (Supplementary

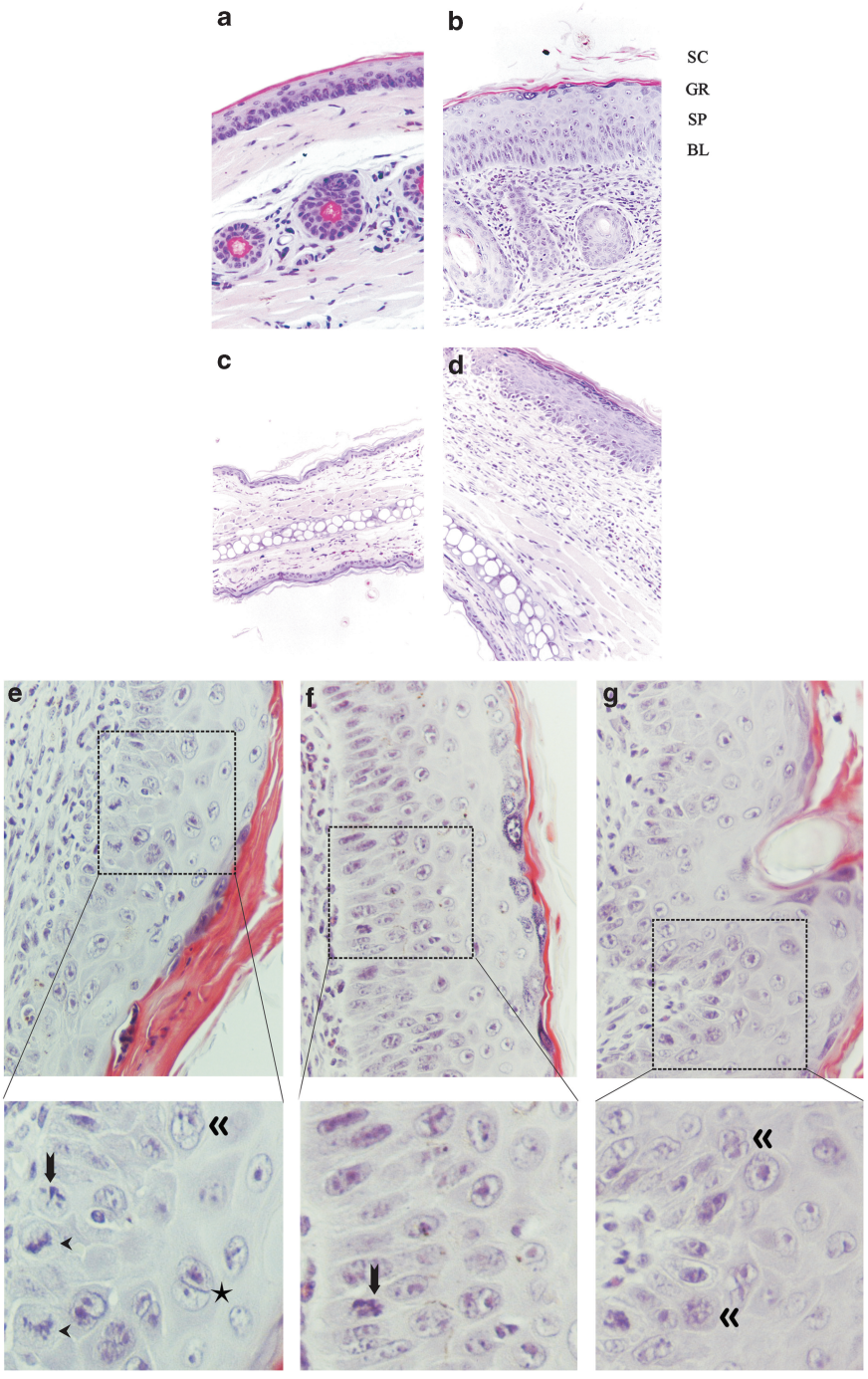

Figure 1. RhoDG26V causes morphological alterations *in vivo*. Histopathological analysis of skin from control (**a**) and transgenic mice (**b**). (**a** and **b**) are from tail skin and (**c** and **d**) from ear. (**e**–**g**) Examples of abnormal mitosis including chromosomal segregation abnormalities and multilobular nuclei are shown. The epidermal cell layers are indicated in (**b**), BL = basal layer, SP = spinous layer, GR = granular layer, SC = stratum corneum. H&E on paraffin sections (**a** and **b**): × 200 and (**e**–**g**): × 100. Typical mitoses (➢), atypical mitoses (⇓), multilobulated cells («) and binucleate cells (★).

Figure 1e), whereas in control mice were restricted to the basal layer of the epidermis (Supplementary Figure 1d). The hyperplasia was observed in areas without inflammation, ruling out an indirect effect on cell proliferation due to the local release of cytokines. Moreover, focally in some hyperplastic lesions we have observed atypical epithelial changes, such as multinucleated and multilobulated cells, nuclear hyperchromasia, increased number of mitosis including atypical forms (Figures 1e–g; quantitation in Supplementary Figure 1f). However, the animals did not develop malignancies even as they aged.

Hyperplasia of the transgenic mice epidermis was associated with perturbed differentiation. Indeed, whereas some markers were expressed correctly, others exhibited altered expression patterns. Thus, Filaggrin and K1 protein were expressed correctly in the granular and suprabasal layers of the epidermis of control (Supplementary Figures 2a and c) and transgenic animals (Supplementary Figures 2b and d), respectively. On the contrary, expression of the K6 protein was restricted to hair follicles in control mice (Supplementary Figure 2e), but was expressed throughout the epidermis of transgenic skin (Supplementary Figure 2f), as observed in hyperplastic, neoplastic and psoriatic skin.[20] The strongest manifestation of altered differentiation was, however, the expanded expression of K14 protein throughout the epidermal layers of transgenic skin (Supplementary Figure 2h) contrary to restricted expression of K14, as expected, to the basal layer and hair follicles of control mice (Supplementary Figure 2g). Extended pattern of K14 expression has been previously reported in many cases of epidermal hyperplasia.[21] Likewise, the K14 promoter-driven RhoDG26V was expressed throughout the epidermis in transgenic mice (Supplementary Figure 2j), instead of being restricted to the basal layer. This result suggests that K14 promoter-driven RhoDG26V expression inhibits silencing of the K14 promoter and induces the proliferation of basal layer cells allowing their expansion to the suprabasal layers.

RhoD is required for S-phase entry

To further investigate the role of RhoD in proliferation, we carried out proliferation assays in cell culture. RhoD is ubiquitously expressed; therefore, we used endothelial cells as they are well synchronized, can be induced to proliferate with growth factors and express RhoD. In agreement with the RhoDG26V-induced hyperplasia of transgenic skin, overexpression of wild-type RhoD (Ad-myc-RhoDWT) in human umbilical vein endothelial (HUVE) cells enhanced both basal and vascular endothelial growth factor (VEGF)-induced proliferation, whereas overexpression of a dominant-negative mutant of RhoD (Ad-myc-RhoDT31N) inhibited both basal and VEGF-induced thymidine incorporation (Figure 2a). Similar results were obtained in primary Bovine brain endothelial cells (data not shown). Furthermore, in a human keratinocyte cell line, HaCaT cells, overexpression of wild-type RhoD enhanced epidermal growth factor-induced cell proliferation (Supplementary Figure 3A, a and b). RhoDG26V did not exhibit any stimulatory effect on proliferation *in vitro*, probably due to increased apoptosis (Supplementary Figure 3B, a). Indeed, RhoDG26V-expressing transgenic mice did exhibit a degree of apoptosis, whereas no apoptosis was visible in the epidermis of control littermates (data not shown).

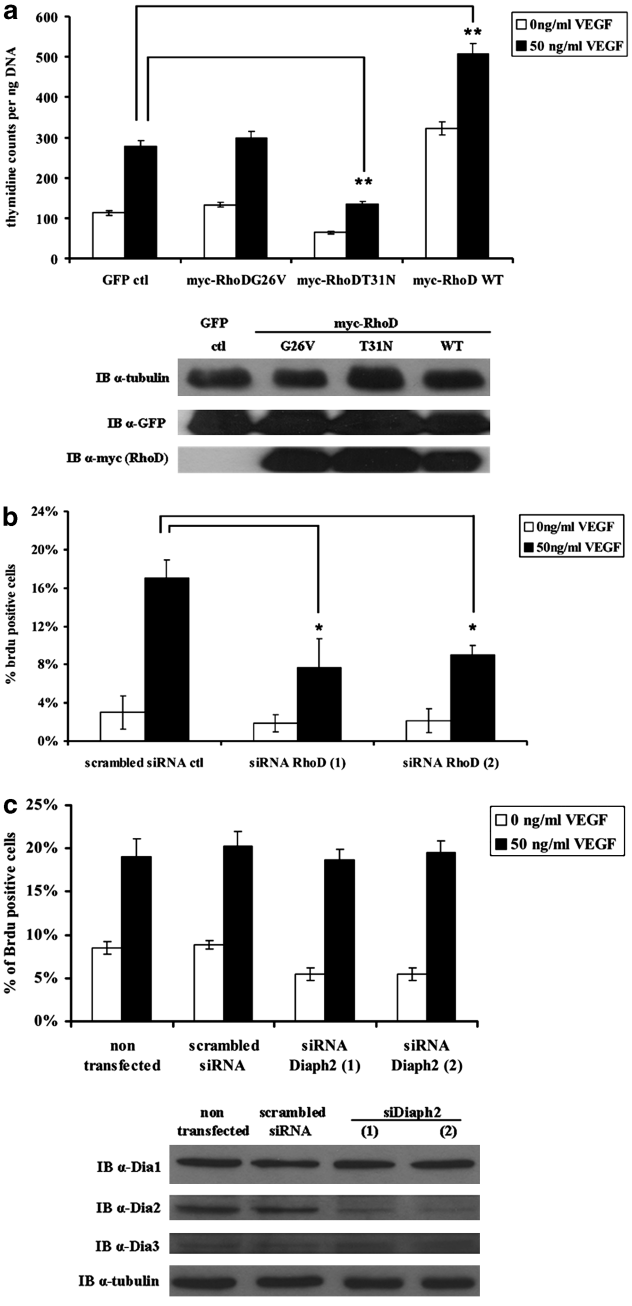

Figure 2. RhoD alters endothelial cell proliferation *in vitro* and this effect is not mediated through hDia2C. (**a**) HUVE cells were infected with Ad-GFP, Ad-myc-RhoDWT, Ad-myc-RhoDG26V or Ad-myc-RhoDT31N for 24 h, then thymidine incorporation, proliferation assay, fluorimetry for DNA content and indirect immunofluorescence and western blot analysis were performed as indicated in Materials and methods. Graphs indicate percentage of thymidine incorporation normalized to total DNA content ± s.d. derived from triplicate samples. The experiment was performed twice. $^{**}P < 0.005$ for RhoDT31N and RhoDWT compared with control GFP>. Western blot analysis indicating expression levels of all RhoD mutants and GFP control virus. (**b**) HUVE cells were either transfected with 20 nM of the scrambled siRNA control or with each of the two RhoD siRNAs and BrdU incorporation in the absence and presence of VEGF was performed as described.[44] Graphs indicate percentage of BrdU incorporation ± s.d. derived from triplicate samples. The experiment was performed three times. $^{*}P < 0.01$ for siRNA RhoD oligos 1 and 2. The knockdown efficiency of the two RhoD siRNAs was tested by qRT–PCR in RNA isolated from HUVE cells transfected for 72 h with 20 nM siRNAs. GAPDH mRNA was used to normalize the values. (**c**) HUVE cells were either transfected with 20 nM of the scrambled siRNA control or with each of the two Diaph2 siRNAs and BrdU incorporation in the absence and presence of VEGF was performed as outlined in Bellou *et al*.[44] Graphs indicate percentage of BrdU incorporation ± s.d. derived from triplicate samples. The experiment was performed twice. The specificity and efficiency of the two Diaph2 siRNAs is shown by western blot analysis.

Knockdown of RhoD, using two siRNAs, resulted in a statistically significant decrease of basal and VEGF-induced BrdU incorporation in HUVE cells compared with cells transfected with the scrambled siRNA control (Figure 2b). Both siRNAs decreased dramatically the expression of the RhoD mRNA (Supplementary Figure 4A, a) and protein levels (Supplementary Figure 4A, b) of the endogenous or overexpressed RhoD, respectively. FACS analysis of RhoD-depleted HeLa and HUVE cells revealed a decrease in cells in S phase and an accumulation in G1, confirming that RhoD knockdown inhibits G1-S progression (Supplementary Figure 3B, b and c).

Importantly, the two siRNAs against RhoD increased the levels of RhoB with marginal effect on the levels of RhoA and RhoC mRNAs (Supplementary Figure 4B). However, double knockdown of RhoD and RhoB also caused inhibition of BrdU incorporation (Supplementary Figure 4C, a and b), suggesting that the effect of RhoD on cell proliferation is independent of its effect on RhoB. Moreover, RhoD and its mutants did not alter ERK1/2 MAPK (Supplementary Figure 5A, a) and CyclinE/Cdk2 (Supplementary Figure 6A) activity, suggesting that the effect of RhoD on G1-S progression was not mediated via these kinases. Silencing all splice variants of Diaph2 did not affect VEGF-induced BrdU incorporation in HUVE cells (Figure 2c), suggesting that the effect of RhoD on cell cycle did not require HDia2C, a splice variant of Diaph2, which is a known effector of RhoD.[17] In conclusion, RhoD is important for S-phase entry and a known RhoD effector HDia2C does not mediate this effect.

Identification of Diaph1 as a RhoD-interacting protein

To identify RhoD-interacting proteins having a role in S and/or M-phase regulation, we used the yeast two-hybrid system. The screen was functional as hDia2C,[17] a known RhoD effector, was identified as an interacting protein. Clones were categorized according to their Predicted Biological Score (PBS) as described.[22] Among the results, the screen identified 36 yeast two-hybrid clones of PBS category A that mapped to the GTP-binding Domain of Diaph1, a protein related to hDia2C and was therefore selected for further analysis. The interaction of RhoD and Diaph1 was confirmed using both pull-down (Figure 3a) and co-immunoprecipitation (Figure 3b) experiments. The RhoD-Diaph1 interaction was GTP dependent. Indeed, Myc-RhoDG26V (the GTP form) interacted strongly with GST-mDia1, myc-RhoDWT showed a weak interaction, whereas myc-RhoDT31N (the GDP form) did not interact (Figure 3c). In agreement with this result, endogenous Diaph1 protein interacted clearly only with GST-RhoD-GTPγS and not with GST-RhoD-GDP (Figure 3d).

To further confirm the interaction between RhoD and mDia1, we tested the colocalization by confocal microscopy. RhoD is typically localized mainly to early endosomes[14] that are EEA1 positive (Figure 3E, e–h), whereas wild-type mDia1 (auto-inhibited conformation) exhibits a diffuse cytoplasmic staining,[23] Figure 3E, a–d. Upon co-transfection of HUVE cells with GFP-mDia1 and myc-RhoDG26V, we observed a strong recruitment of GFP-mDia1 onto RhoDG26V-positive endosomes (Figure 3E, i–l). Taken together, our data suggest that RhoD forms a complex with Diaph1 both *in vitro* and *in vivo* and is recruited on RhoD-positive endosomes. These results confirm that Diaph1 is a genuine RhoD-interacting protein.

RhoD affects proliferation through Diaph1

We next attempted to correlate the RhoD-mDia1 interaction with the stimulation of proliferation caused by RhoDWT overexpression. Toward this end, we knocked down, using siRNAs, Diaph1, Diaph2 and Diaph3 in HUVE cells, which were subsequently infected either with Ad-GFP or with Ad-myc-RhoDWT. Despite the fact that all siRNAs worked well (Figure 4b), only the Diaph1 siRNA could inhibit the increased cell proliferation induced upon overexpression of RhoDWT (Figure 4a). Depletion of Diaph1, by three different silencing siRNAs, exhibited essentially similar results (Figures 4c and d). Therefore, we conclude that the increased proliferation induced by RhoD is mediated through its effector protein Diaph1.

RhoD localizes to the pericentrosomal region and causes centrosomal amplification

Overexpression of RhoDG26V induced in HUVE cells, as well as in several other cells lines (HeLa, BHK, NIH3T3 and BBCE), significant nuclear fragmentation (Figure 5B, a–c) and multinucleation (Figure 5B, d–f) compared with control (Figure 5A, a–c). Similar changes were also observed in the transgenic mouse skin (Figure 1, e–g). Nuclear fragmentation and multinucleation occurred independently from each other as seen by video microscopy of Ad-myc-RhoDG26V-infected HUVE cells (video as Supplementary Movie 1). The binucleate cells were $\sim$10% while cells with nuclear fragmentation reached 40% at 48 h (Figure 5c). Importantly, HeLa cells overexpressing RhoDG26V also exhibited chromosome misalignment and formed multiple spindles during metaphase (Figure 5D, a and b). Approximately 15% of the cells exhibited this phenotype, which was not observed in control HeLa cells (Figure 5D, graph) or cells expressing the wild-type or dominant-negative RhoD (data not shown). This phenotype was not mediated through HDia2C, as depletion of this molecule did not inhibit the RhoDG26V effect (Supplementary Figure 5A, b).

As multiple spindle formation could derive from centrosomal amplification, we investigated whether RhoD exhibited a centrosomal localization and/or was associated with defects in centrosome duplication. Indeed, RhoDWT and RhoDG26V were colocalized with α-tubulin around one of the GFP-centrin couples of the G2-phase cells (Figure 6a), suggesting a pericentrosomal location around one of the centrosomes. RhoDG26V exhibits minimal colocalization with PCM1 (Figure 6b), a component of centriolar satellites.[24] Moreover, the considerable colocalization of RhoDG26V with internalized transferrin (Figure 6c) in the

Figure 3. RhoD interacts with mDia1. (**A**) HEK 293 cell extracts transiently expressing myc-RhoDG26V were incubated with GST alone, GST-GBD mDia1 or GST-GBD hDia2C, as a positive control, for 4 h at 4 °C with rotation as described.[46] Lysis buffer: 50 mM Tris pH 7.4, 5 mM $MgCl_2$, 0.1 mM DTT, 150 mM NaCl, 0.5% NP-40. The beads were washed five times with assay buffer before eluting the bound proteins with SDS-sample buffer. Bound proteins were subjected to 12% SDS–PAGE. The upper panel is a Coomassie staining of the GST fusion proteins and GST control, center panel is the myc-RhoDG26V bound to the beads and lower panel are the total inputs. (**B**) HEK 293 cells were co-transfected with myc-RhoDG26V and FLAG-mDia1WT or FLAG-hDia2c for 24 h. Co-immunoprecipitation was carried out as described[46] using α-FLAG and control IgG antibodies. Lysis buffer: 0.1% NP-40, Tris pH 7.4 50 mM, 5 mM $MgCl_2$, NaCl 150 mM, supplemented with protease inhibitor cocktail tablet (Roche). Panel 3 shows myc-RhoDG26V co-immunoprecipitated with mDia1 and hDia2C. For detection of RhoD and mDia1 or hDia2C, rabbit α-RhoD and mouse α-FLAG were used, respectively. RhoD interaction with mDia1 is nucleotide dependent. (**C**) HEK 293 cell extracts transiently expressing myc-RhoDWT, myc-RhoDG26V or myc-RhoDT31N were incubated with GST-GBD hDia2C and processed as outlined in (**A**). RhoD interacts with endogenous Diaph1 in a GTP-dependent fashion. (**D**) GST-RhoDWT was loaded with either GDP or GTPγs and incubated with human placental lysate as described.[47] RhoDG26V recruits mDia1 to the early endocytic compartment. (**E**) HUVE cells were transiently transfected with myc-RhoDG26V and FLAG-mDia1 and the appropriate vector controls and processed for immunofluorescence. GFP was visualized directly (shown in green), myc-RhoDG26V was visualized using the 9E10 α-myc monoclonal antibody and is shown in red, and EEA1 was visualized using an α-EEA1 antibody and is shown in blue. Size bar is 10 microns.

pericentriolar region hints at a possible implication of RhoD in the centrosome function (mitotic spindle formation/chromosome segregation) from the perinuclear recycling compartment.

Overexpression of RhoDG26V in HUVE cells lead to formation of multiple centrioles (Figure 7A, a–c) compared with control cells (Figure 7A, d and e). Approximately 30% of the RhoD over-expressing cells exhibited increased centriole numbers compared with 10% in control cells (Figure 7b). This was also the case in HaCaT cells where overexpression of RhoDG26V increased centriole numbers to ~22% compared with 12% in control (Supplementary Figure 5B, a). Furthermore, upon expression of dominant-negative RhoDT31N or endogenous RhoD depletion, the number of HUVE cells exhibiting <2 centrin-positive structures increased in a statistically significant manner compared with controls (Figure 7c), this was also the case in HaCaT cells (Supplementary Figure 5B, b and c). In the same context, we have observed less endogenous γ-tubulin-positive structures (centrosomes) in RhoD-depleted cells (Figure 7D). Electron microscopy

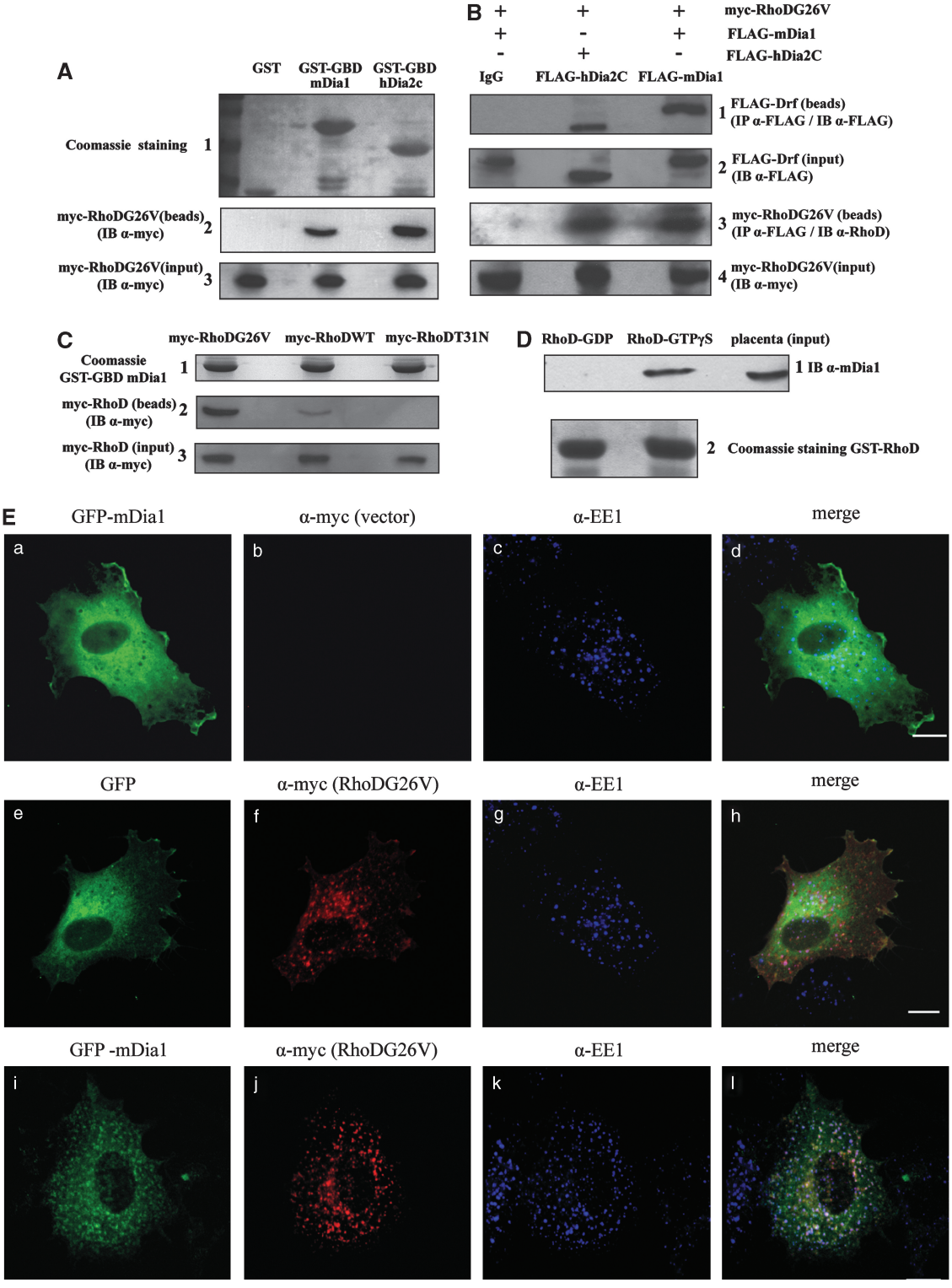

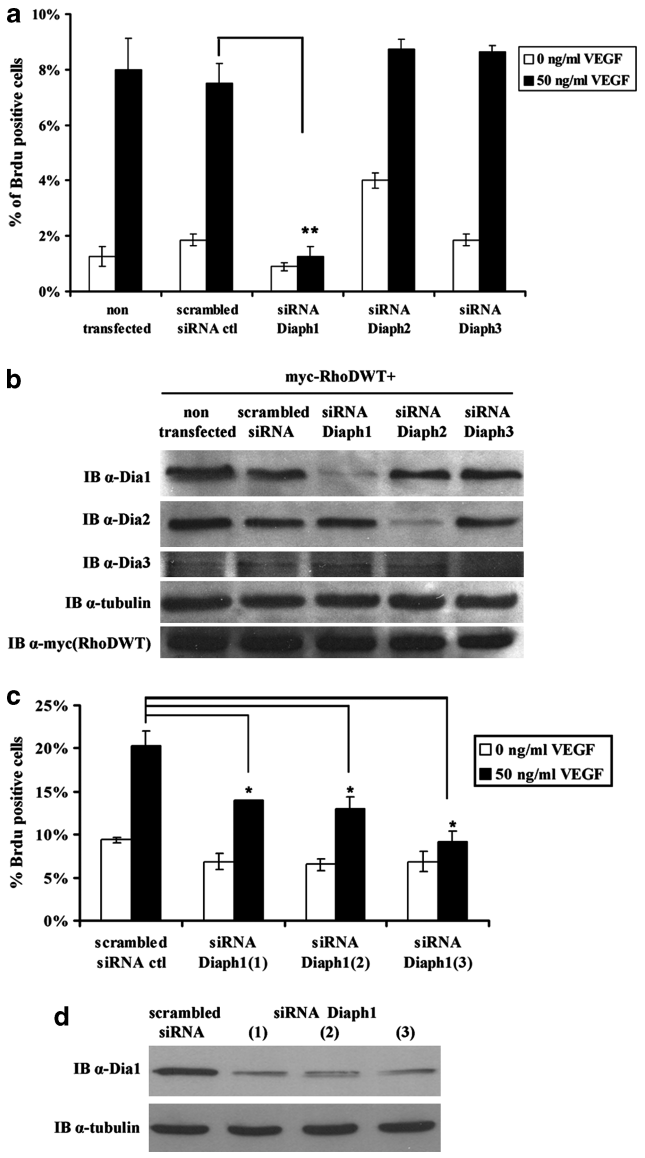

Figure 4. The effect of RhoD on cell proliferation is mediated through mDia1. (**a**) HUVE cells were transfected with scrambled, Diaph1, Diaph2 or Diaph3 siRNAs at 20 nM for 24 h. The cells were then infected with Ad-myc-RhoDWT for 24 h and BrdU incorporation in the absence and presence or VEGF was carried out as in Bellou *et al*,[44] $^{**}P<0.005$. The specificity and efficiency of the siRNAs and expression of RhoDWT is shown in (**b**) with tubulin as a loading control. (**c**) Use of three different siRNAs against Diaph1 exhibited similar results, $^{*}P<0.05$. (**d**) Knockdown of Diaph1 protein levels.

confirmed that several HUVE cells overexpressing RhoDG26V exhibited increased number of centrioles (Figure 7E, b), whereas none of the control cells exhibited this phenotype (Figure 7E, a). Electron microscopy of RhoD siRNA transected cells confirmed the absence of centrioles (data not shown). These results clearly suggest that RhoD has a regulatory role in centrosome duplication and its overactivation leads to centrosome amplification. However, this effect seems to be mediated via other effectors as depletion of Diaph1 did not inhibit the centriole overduplication induced by RhoDG26V (data not shown).

Next, we carried out a centriole overduplication assay using p53-deficient U2OS cells. In this assay, the cell cycle is inhibited by aphidicolin treatment and allows uncoupling of the cell cycle from the centrosome cycle.[25] The assay revealed that the effect of RhoD on centriole duplication was direct, being independent from the effect of RhoDG26V on cell cycle. Indeed, RhoDT31N inhibited centriole overduplication by $\sim$40% compared with control, whereas RhoDG26V further stimulated centriole duplication by $\sim$25% (Figure 7f), both effects being statistically significant. Interestingly, RhoD appeared to be involved in Plk4-induced centrosome duplication. In HeLa cells expressing HA-Plk4 under the tetracycline inducible promoter,[26] expression of RhoDT31N decreased the percentage of cells with >4 centrioles decreased by $\sim$25% inhibiting the Plk4-induced multiplication of centrin-positive structures (Figure 7g). The recruitment of PLK4 to the centrioles was however unaffected by the expression of RhoDT31N (data not shown). The strong association of the centrosome duplication phase with Plk2[27] and ROCKII[28] prompted us to study their possible interplay with RhoD. RhoD and mutants did not affect Cdk2/Cyclin E nor PLK2 activity (Supplementary Figures 6A and B, respectively), and siRNA of ROCKII (Supplementary Figure 6D) did not reverse RhoD induced centriole overduplication.

The above results revealed that the phenotypic alterations of RhoDG26V extended until the very end of mitosis. We therefore investigated the activation state of RhoD during the different stages of M phase. We found that RhoD was activated during mitosis with a peak at 30 min, corresponding to prometaphase. The activity decreased as the cells progressed to later stages of mitosis and was almost abolished during the exit from cell division (Supplementary Figure 7A). The punctate (endosomal) localization of RhoDWT did not change during mitosis throughout division (Supplementary Figure 7B, a). The endosomal nature of the punctate localization was confirmed by ample colocalization of RhoDWT with internalized FITC-transferrin (Supplementary Figure 7B, b). The dominant-negative mutant remained cytosolic (data not shown), whereas the G26V mutant exhibited localization essentially similar to the WT protein (data not shown).

DISCUSSION

Overexpression of RhoDG26V in the epidermis of transgenic mice lead to increased thickness of all layers of epidermis associated

Figure 5. RhoDG26V causes nuclear fragmentation, multinucleation and mitotic abnormalities. (**A**) HUVE cells were infected with Ad-GFP for 24 h and processed for immunofluorescence as outlined in Bellou *et al*.[44] DNA was visualized using YOYO and shown in green, GFP was visualized using an α-GFP antibody (shown in red). (**B**) Multinucleation and fragmentation induced upon overexpression of RhoDG26V. HUVE cells were infected with Ad-myc-RhoDG26V for 24 h and processed for immunofluorescence. DNA was visualized using YOYO and shown in green, myc-RhoDG26V was visualized using the 9E10 α-myc monoclonal antibody (shown in red). (**C**) Quantitation of the effects of RhoDG26V on nuclear multinucleation and fragmentation at different time points following infection are shown. (**D**) Mitotic abnormalities upon overexpression of RhoDG26V. (a) and (b) represent two examples of abnormal mitotic phenotypes upon expression of RhoDG26V. HeLa cells at 50% confluence were infected with either Ad-GFP or Ad-myc-RhoDG26V for 12 h. Cells were then treated with nocodazole (40 ng/ml) for a further 10 h. Mitotic cells were collected by mechanical shaking, released from nocodazole block by washing twice with fresh medium, incubated for a further 1 h and plated on polylysine-coated coverslips. Cells were then processed for immunofluorescence. DNA was visualized using YOYO and shown in green, myc-RhoDG26V was visualized using the 9E10 α-myc monoclonal antibody and is shown in red, and tubulin was visualized using an α-tubulin antibody and shown in blue. Arrows indicate the presence of multiple spindles. The percentage of abnormal cell division upon expression of Ad-GFP or Ad-myc-RhoDG26V as defined by abnormal spindle formation or chromosomal segregation is shown. A quantitation of chromosome misalignment upon RhoDG26V expression is shown in the graph. $^{*}P<0.05$, $^{**}P<0.005$.

with decreased differentiation. These changes were reminiscent of hyperplastic, neoplastic and psoriatic skin.[20] However, neither RhoD nor RhoDG26V supported growth of NIH3T3 or BHK cells in soft agar (data not shown), suggesting that RhoD does not cause transformation alone. RhoDWT stimulated both basal and VEGF-induced proliferation in primary endothelial cells, whereas

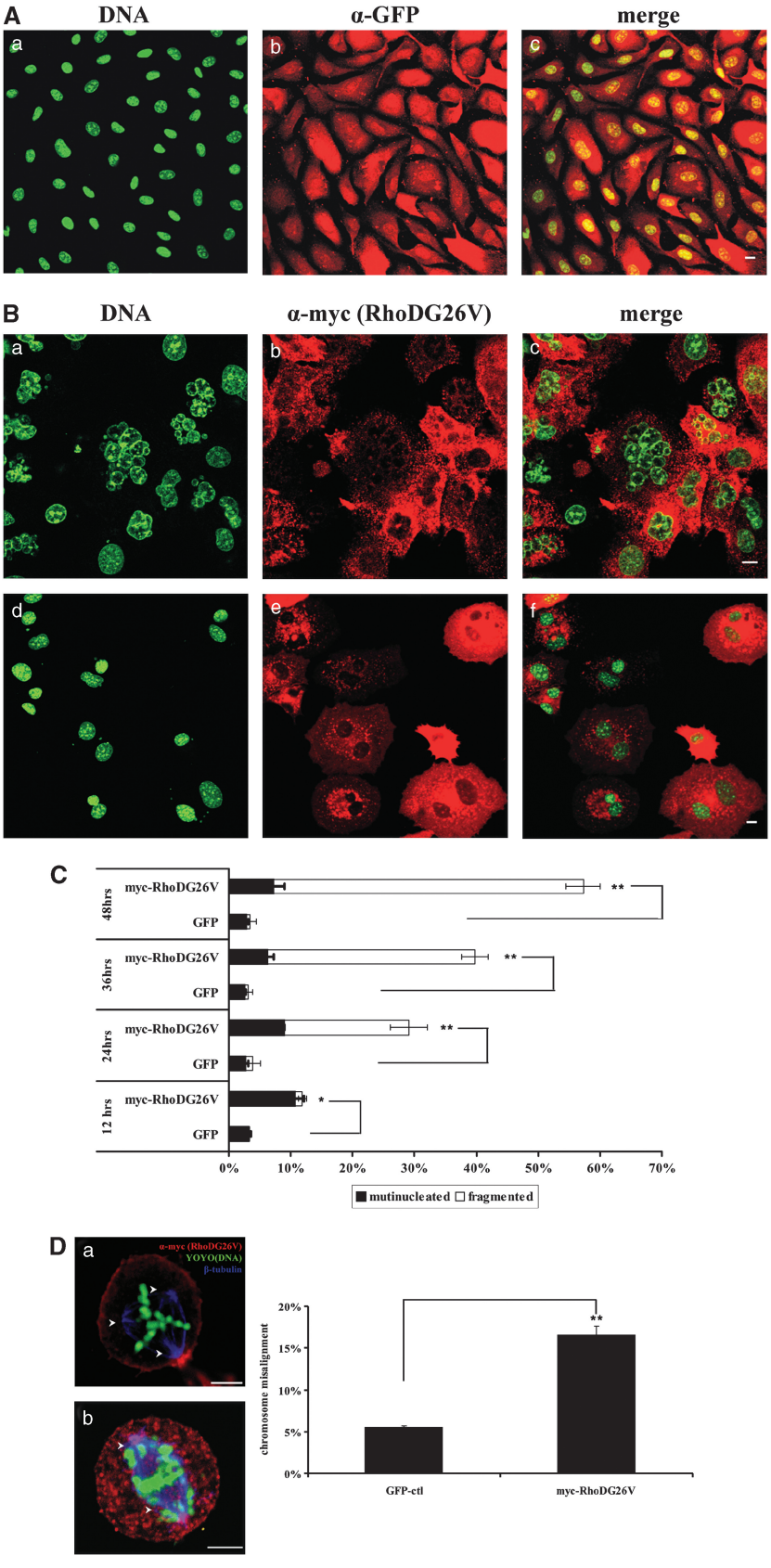

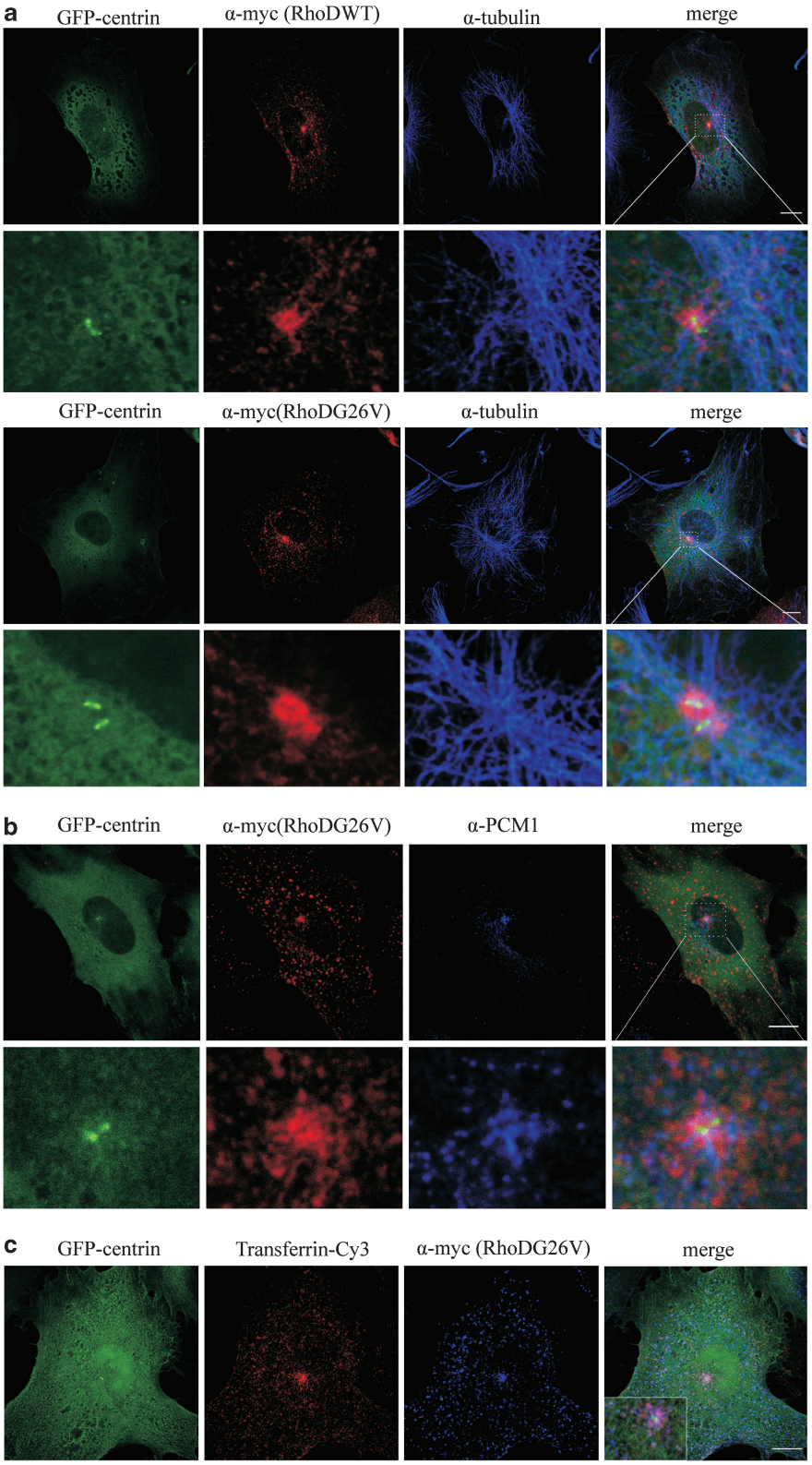

Figure 6. RhoD encircles centrosomes. (**a**) RhoDG26V surrounds one of the two centrin-positive couples. HUVE cells were infected with GFP-centrin and myc-RhoDG26V. Twenty-four hours post transfection, cells were processed for GFP-centrin, myc-RhoDWT or G26V (red-TRITC) and endogenous α-tubulin (blue-CY5). (**b**) RhoDG26V does not colocalize with PCM1-positive centrosome granules. HUVE cells were transfected with myc-RhoDG26V for 24 h and incubated with α-myc (myc-RhoDG26V) and α-PCM1 abs. (**c**) RhoDG26V colocalizes with transferrin-positive perinuclear compartment. HUVE cells were infected with GFP-centrin and myc-RhoDG26V. Twenty-four hours post transfection, cells were starved for 1 h (0% FBS), incubated with transferrin-CY3 for 45 min, fixed and Myc-RhoDG26V was visualized using the 9E10 α-myc monoclonal antibody and is shown in blue. Size bars are 10 microns.

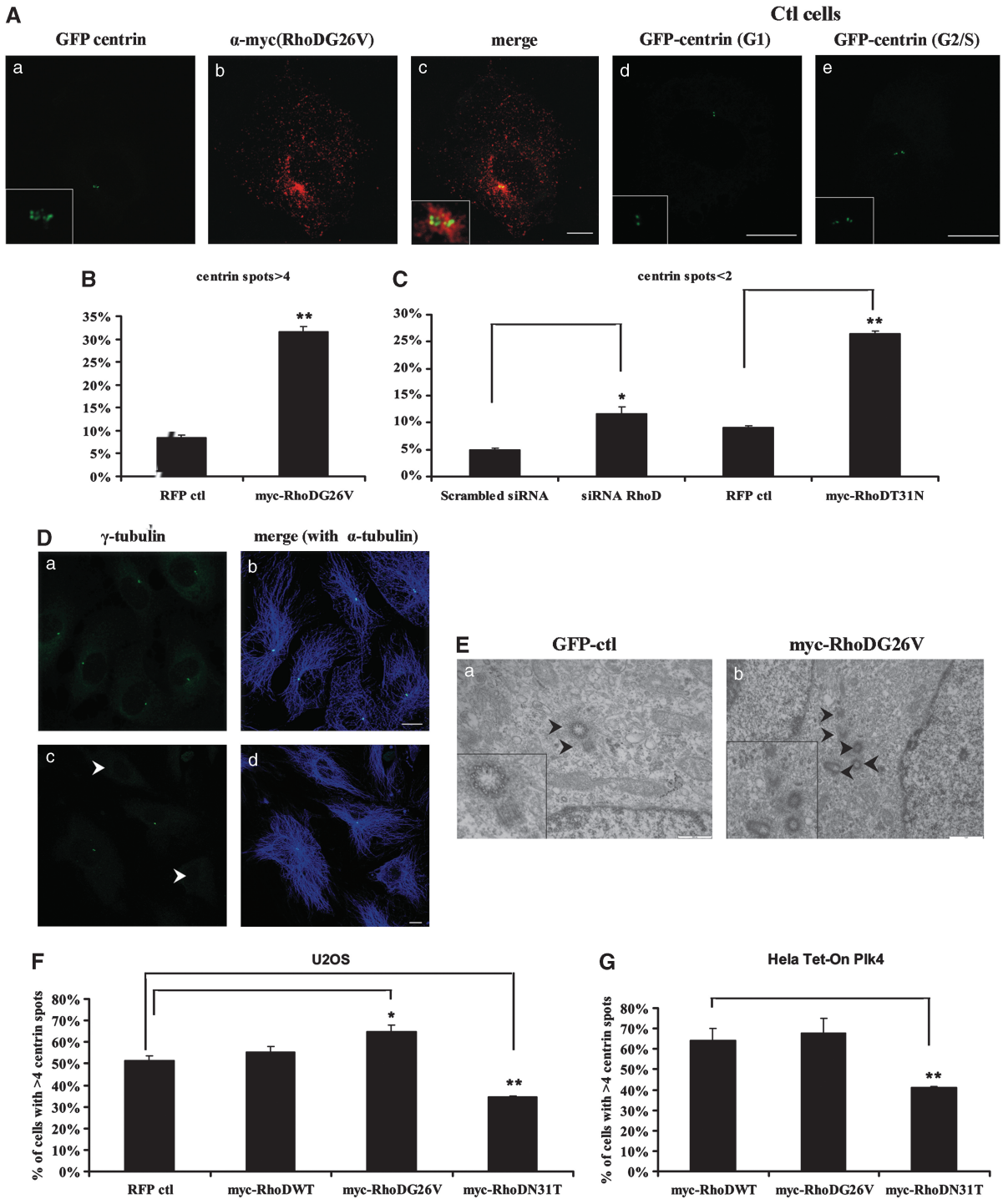

Figure 7. Activation of RhoD increases, while RhoD silencing decreases, centrosome numbers. (**A**) HUVE cells infected with GFP control (d and e) or Ad-myc-RhoDG26V for 24 h (a–c). Quantitation of GFP-centrin-positive structures revealed centriole amplification following constitutive activation of RhoD (**B**) and decrease in the centriole structures upon knockdown of the gene (48 h) or expressing the dominant-negative form of RhoD (T31N) for 24 h (**C**). RFP is red fluorescent protein used as a transfection control. Myc-RhoDG26V was visualized using the 9E10 α-myc monoclonal antibody and is shown in red. (**D**) Endogenous γ-tubulin staining after knockdown of *RHOD* yielded cells lacking centrosomes. (a) Scrambled siRNA transfected HUVEC show normal endogenous γ-tubulin staining. (b) The merged image with α-tubulin staining. (c) RhoD depletion yields cells that lack centrosomal staining. (d) Merged with α-tubulin staining. (**E**) Electron microscopy of HUVE cells infected with Ad-GFP control (a) and Ad-myc-RhoDG26V (b). Subconfluent HUVE cells were either transfected with siRNAs for 48 h or infected with adenoviruses expressing GFP or myc-RhoD mutants for 30 h. After washing with PBS, cells were fixed with 2% glutaraldehyde for 1 h at RT and then processed for epon embedding *in situ*. Sections were cut parallel to the culture substratum and all analyses of centriole morphology were carried out by comparing sections passing through the perinuclear region of the cell as characterized by abundant Golgi profiles arrowheads indicate centriolar structures. (**F**) Centrosome duplication assay in U2OS and HeLa-Tet-on Plk4 (**G**) indicates that the dominant-negative form of RhoDT31N inhibits centrosome amplification. $^{*}P<0.05$, $^{**}P<0.005$. U2OS and HeLa-Plk4 cells were transfected for 30 h with plasmids expressing GFP-centrin and RhoD mutants. Centrosome duplication assay was performed as described.[26]

RhoDG26V did not exhibit a stimulatory effect on proliferation *in vitro*, due to increased apoptosis as a consequence of nuclear fragmentation and multinucleation. Nevertheless, overexpression of the dominant-negative RhoDT31N mutant and RhoD silencing by three independent siRNAs blocked G1-S progression, leaving no doubt that RhoD is required for G1-S progression and cell proliferation. Other Rho proteins activate G1/S-phase progression too. RhoA activates cyclinE/CDK2,[29] whereas Rac and Cdc42 GTPases facilitate G1/S-phase progression[30,31] either by enhancing cyclin D1 transcription/translation or by downregulating p27kip1 and p21cip1 in mitogen-stimulated cells, reviewed in Villalonga and Ridley.[32] RhoDWT and RhoDG26V did not affect the activity of cyclin E/CDK2 excluding this mechanism.

Gene-silencing experiments revealed that Hdia2C, a known effector of RhoD, did not mediate the effect of RhoD on G1/S-phase progression. In this context, we have identified Diaph1 as a novel RhoD-interacting protein using a two-hybrid yeast screen. The RhoD-Diaph1 interaction was fully validated both biochemically and microscopically. It has been previously shown that suppression of mDia1 (the mouse homolog of Diaph1) inhibits G1 progression[7] by decreased expression of the F-box protein Skp2 that controls a rate-limiting step in the ubiquitin-mediated degradation of p27.[33] As a consequence, Diaph1 appeared to be an excellent candidate to mediate the effect of RhoD on G1/S-phase progression. Indeed, siRNA knockdown of Diaph1, but not Diaph2 or Diaph3, decreased dramatically RhoDWT-induced proliferation (G1-S progression) in HUVE cells. The result strongly suggests that Diaph1 mediates RhoD-induced G1/S-phase progression, probably by enhancing Skp2 levels leading to degradation of the cell-cycle inhibitor p27.[33]

Overexpression of RhoDG26V also caused nuclear fragmentation and multinucleation in many cultured cell lines, as seen in the epidermis of the transgenic mice. Further analysis revealed that nuclear fragmentation was associated with chromosome misalignment and formation of multipolar spindles during metaphase. Because formation of extra spindle poles is compatible with centrosome amplification, we investigated the effect of RhoDG26V on the centrosome cycle. Indeed, overexpression of RhoDG26V caused multiple spindles, in single nucleated cells, via centrin-positive centriole overduplication and not through fragmentation of the pericentriolar material. On the other hand, silencing of the *RHOD* gene yielded cells with no visible centrosomes. These results suggested a regulatory role of RhoD on centrosome integrity and centrosome duplication during the cell cycle. In fact, the centrosome/centriole duplication cycle is coupled with the DNA replication cycle, which is one of the important mechanisms that ensure centrosomes to duplicate only once in a single cell cycle. Co-ordination of these two events is, at least in part, achieved by the late G1 phase-specific activation of cyclin E/CDK2.[34,35]

In this respect, RhoDG26V did not activate cyclin E/CDK2 excluding this kinase from being responsible for RhoD-induced centrosome amplification. In confirmation, silencing of the *ROCK2* gene did not abolish the effect of RhoDG26V on centrosome amplification. Cyclin E/CDK2 phosphorylates NPM/B23 (nucleophosmin),[36,37] which in turn binds to and superactivates ROCK2, a critical event for initiation of centrosome duplication.[28] Likewise, RhoD26V had no effect on Polo-like kinase 2 (Plk2) activation, a kinase that is phosphorylated near G1/S transition. Plk2 also phosphorylates NPM/B23 triggering centrosome duplication.[38,39] Indeed, centriole duplication assays using the p53-deficient U20S cells/aphidicolin assay, which uncouples the cell from the centrosome cycle, indicated a direct effect of RhoD on centrosome duplication. In this assay, RhoDG26V enhanced centrosome amplification, whereas the dominant-negative RhoDT31N exhibited an inhibitory effect.

It has been shown that excess Plk4 kinase activity can lead to the simultaneous formation of multiple centrioles around a single parent, suggesting that Plk4 overexpression creates additional sites on 'duplication-competent' parental centrioles.[40,41] This Plk4 activity is independent of Cdk2 activity, a major difference compared with template-driven centrosome duplication that is linked to the nuclear cycle and requires cyclinA/E/Cdk2.[42] RhoD dominant-negative RhoDT31N reduced the percentage of cells with >4 centrioles induced by Plk4 overexpression by $\sim$40% without recruiting Plk4 to centrosomes. It remains to be determined if there is any direct connection between Plk4 and RhoD in centriole duplication.

Our findings suggest that RhoD is involved in cell proliferation and indeed overexpression of the wild-type protein is sufficient to increase the number of cells progressing through the G1-S phase. The effect on proliferation is associated with decreased differentiation and centrosomal amplification leading to aberrant multipolar spindles and abnormal chromosome segregation. All these aberrations are the hallmarks of the CIN (chromosome instability) phenotype displayed by many cancer cells indicating that further investigation of a possible implication of RhoD in cancer might be warranted.

MATERIALS AND METHODS

Antibodies and recombinant proteins

9E10 antibody was purified as described.[43] α-FLAG M2 antibody (F3165) was from Sigma-Aldrich (St Louis, MO, USA), α-mDia1 antibody (610849) from BD Bioscience, Bedford, MA, USA, α-Dia2 (sc-10892, N-15) from Santa-Cruz Biotechnology Inc. (Santa Cruz, CA, USA), α-Dia3 (H00081624-A01) from Abnova (Abnova, Taipei City, Taiwan) and α-Brdu from Immunologicals Direct. Rabbit (18251) and rat α-tubulin (YOL1/34) were purchased from Abcam (Abcam, Cambridge, UK). Rabbit α-RhoD and α-GFP were from Marino Zerial (MPI-CBG, Dresden, Germany) and Haralabia Boleti (Pasteur Institute, Athens, Greece), respectively. α-Phospho-Erk1/2 (9101) was from Cell Signaling (Cell Signaling Technology Inc., Danvers, MA, USA). All secondary multilabeling antibodies were from Jackson ImmunoResearch Europe Ltd (Jackson ImmunoResearch Laboratories Inc., West Grove, PA, USA). DNA was stained with YOYO (Molecular Probes, InVitrogen, Carlsbad, CA, USA) or PI (Sigma). Human $VEGF_{165}$ was purchased from Immunotools (ImmunoTools GmbH, Friesoythe, Germany) and Rhoteckin-RBD protein GST beads from The Cytoskeleton (The Cytoskeketon, Denver, CO, USA).

Expression plasmids and siRNAs

GST-GBD mDia1, GFP-mDia1 and FLAG-mDia1 were kindly provided by Shuh Narumiya (Kyoto University, Japan). GBD-hDia2C (1–287 aa) was cloned in frame in pGEX-5 and full-length hDia2C (1–1096 aa) in pFLAG-CMV-2. All mutants of mouse RhoD were as previously described.[14] The full-length cDNA clone of human RhoD, hRhoD (IRATp970E084D; ImaGenes, Source BioScience UK Ltd., Nottingham, UK), was N-terminally myc tagged by cloning in pcDNA3-mycN(III), a vector provided by Marino Zerial. GFP-Centrin was a gift from Michel Bornens, Institut Curie, Paris, France. All constructs were verified by DNA sequencing (MWG-BIOTECH AG, Ebersberg, Germany). siRNAs were purchased from Ambion (Ambion-Life Technologies, Carlsbad, CA, USA) as follows: hRhoD: ID 120532 (siRNA 1) and ID 120822 (siRNA 2). Diaph1: ID 242567 (siRNA 1), ID 242568 (siRNA 2) and ID 146614 (siRNA 3). Diaph2: ID 4392420-S4097 (siRNA 1) and ID 4392420-S4095 (siRNA 2). Diaph3: ID 131031 and RhoB: ID 120362. Both hROCKII siRNA (Cat: S102223753) and control scrambled siRNA (all star negative #1027280) were from Qiagen (Hilden, Germany). All plasmids were endotoxin free. DNA oligonucleotides for qRT–PCR were from MWG.

Construction of recombinant adenoviruses

Adenoviruses were constructed using the pADEASY system and amplified as described (http://www.coloncancer.org/adeasy.htm). The expression cassette contains two CMV promoters, one driving RhoD and the second driving the expression of GFP.

Generation of transgenic mice

RhoDG26V was cloned into the K14 expression cassette provided by Elaine Fuchs (Howard Hughes Medical Institute, University of Chicago, IL, USA).

Transgenic mice were generated by BRL, Switzerland. All animal studies were in compliance with the German regulations.

Histological analysis fixation and immunofluorescence

Tissues from the mice were fixed in buffered formalin and paraffin embedded. Sections were stained with hematoxylin/eosin (H&E). α-PCNA staining was performed using a monoclonal antibody (clone PC10, DAKO North America Inc., Carpinteria, CA, USA). K 1, 6 and filaggrin antibodies (BABCO, Berkeley Antibody Company (BAbCO), Richmond, CA, USA) were used on paraffin-embedded sections. K14 antibody (BABCO) was used on methanol fixed cryosections. The sections were viewed using either a Leica TCS-SP scanning confocal microscope (Leica Microsystems GmbH, Mannheim, Germany) or a Leica TCS SP5 confocal microscope and objectives HCX PL APO CS 100.0 × 1.4 oil and HCX PL APO CS 63.0 × 1.4 oil UV. Prolong antifade mounting medium or Mowiol/DABCO were used.

Cell culture

HUVE cells were isolated and maintained as previously described.[44] HEK 293 and HeLa, HaCaT or U2OS cells were cultured in RPMI-1640 and DMEM medium, respectively, both containing 10% FBS and maintained at 5% CO_2.

Cell transfection

For immunoprecipitation and pull-down assays, HEK 293 cells were transfected with FuGENE 6 (Roche, Basel, Switzerland.) or Lipofectamine 2000 (Invitrogen, Carlsbad, CA, USA) according to manufacturer's instructions or infected with adenoviruses at multiplicity of infections of 5.

For the knockdown experiments, HUVE cells or BBCEs and HaCaT cells were transfected with 20 and 40 nM siRNA, respectively, as described.[44] After 48–72 h, cells were fixed, infected or lysed.

For localization studies, HUVE cells were seeded onto collagen-coated 11-mm glass coverslips, transfected with various constructs, fixed and processed for immunofluorescence and imaging as described,[44,45] see also Histological analysis fixation and immunofluorescence section.

RNA isolation and quantitative real-time RT–PCR

Total RNA was isolated and qRT–PCR was carried out as described.[44] The oligos used for amplification of specific mRNAs are outlined in Supplementary information.

^{3}H-TdR incorporation

HUVE or HaCaT cells were infected with adenoviruses and 24 h later cells were processed as described.[45] Twenty-four hours post HUVE cell infection, a 6-h starvation with 5% FCS was performed followed by 50 ng/ml VEGF for 24 h for HUVE cells, whereas HaCaT cells were serum starved (0% FCS) for 3 h followed by the addition of 20 ng/ml epidermal growth factor for 24 h. In all, 1 μC/ml [^{3}H] was added 6 h before fixation.

For normalization of the values, the same experiment was performed without the final pulse with ^{3}H-TdR. Cells were washed with PBS, lysed with 0.1% SDS, sonicated and 5 μl of the lysates was incubated with 0.5 μg/ml Hoechst 33258 (Sigma). After 5-min incubation, fluorescence was estimated at excitation λ355 nm, emission λ460 nm, and compared with standard DNA controls. Measurements were carried out using a Hitachi F2500 Spectrophotometer (Hitachi Ltd, Tokyo, Japan).

CONFLICT OF INTEREST

The authors declare no conflict of interest.

ACKNOWLEDGEMENTS

We thank the confocal laser microscope facility of the University of Ioannina for the use of the Leica TCS-SP confocal microscope. We thank George Bartholomatos for FACS analysis; Zoi Lygerou, University of Patras, Greece for critical reading of the manuscript; George Keech for excellent animal husbandry; and Angelika Giner for expert technical assistance. This work was supported by a Research Training Network grant (to MZ and CM) of the European Commission (contract no: HRPN-CT-2000-00081). CM was supported by a short-term EMBO fellowship. MS was supported by the Postgraduate Master's Program of Biotechnology of the University of Ioannina funded by the Ministry of Education and Religious Affairs of Greece. AK was supported by the PENED 03EΔ688 program, which was co-financed by E.U.-European Social Fund (75%) and the Greek Ministry of Development-GSRT (25%). RGP was supported by grants from the National Health and Medical Research Council of Australia.

REFERENCES

1 Jaffe AB, Hall A. Rho GTPases: biochemistry and biology. *Annu Rev Cell Dev Biol* 2005; **21**: 247–269.
2 Sit ST, Manser E. Rho GTPases and their role in organizing the actin cytoskeleton. *J Cell Sci* 2011; **124**(Part 5): 679–683.
3 Nagasaki T, Gundersen GG. Depletion of lysophosphatidic acid triggers a loss of oriented detyrosinated microtubules in motile fibroblasts. *J Cell Sci* 1996; **109**: 2461–2469.
4 Cook TA, Nagasaki T, Gundersen GG. Rho guanosine triphosphatase mediates the selective stabilization of microtubules induced by lysophosphatidic acid. *J Cell Biol* 1998; **141**: 175–185.
5 Palazzo AF, Cook TA, Alberts AS, Gundersen GG. mDia mediates Rho-regulated formation and orientation of stable microtubules. *Nat Cell Biol* 2001; **3**: 723–729.
6 Wen Y, Eng CH, Schmoranzer J, Cabrera-Poch N, Morris EJ, Chen M *et al.* EB1 and APC bind to mDia to stabilize microtubules downstream of Rho and promote cell migration. *Nat Cell Biol* 2004; **6**: 820–830.
7 Mammoto A, Huang S, Moore K, Oh P, Ingber DE. Role of RhoA, mDia, and ROCK in cell shape-dependent control of the Skp2-p27kip1 pathway and the G1/S transition. *J Biol Chem* 2004; **279**: 26323–26330.
8 Carreira S, Goodall J, Denat L, Rodriguez M, Nuciforo P, Hoek KS *et al.* Mitf regulation of Dia1 controls melanoma proliferation and invasiveness. *Genes Dev* 2006; **20**: 3426–3439.
9 Downward J. Targeting RAS signalling pathways in cancer therapy. *Nat Rev* 2003; **3**: 11–22.
10 Sahai E, Marshall CJ. RHO-GTPases and cancer. *Nat Rev* 2002; **2**: 133–142.
11 Preudhomme C, Roumier C, Hildebrand MP, Dallery-Prudhomme E, Lantoine D, Lai JL *et al.* Nonrandom 4p13 rearrangements of the RhoH/TTF gene, encoding a GTP-binding protein, in non-Hodgkin's lymphoma and multiple myeloma. *Oncogene* 2000; **19**: 2023–2032.
12 Schnelzer A, Prechtel D, Knaus U, Dehne K, Gerhard M, Graeff H *et al.* Rac1 in human breast cancer: overexpression, mutation analysis, and characterization of a new isoform, Rac1b. *Oncogene* 2000; **19**: 3013–3020.
13 Singh A, Karnoub AE, Palmby TR, Lengyel E, Sondek J, Rac1b Der CJ. a tumor associated, constitutively active Rac1 splice variant, promotes cellular transformation. *Oncogene* 2004; **23**: 9369–9380.
14 Murphy C, Saffrich R, Grummt M, Gournier H, Rybin V, Rubino M *et al.* Endosome dynamics regulated by a Rho protein. *Nature* 1996; **384**: 427–432.
15 Murphy C, Saffrich R, Olivo-Marin J-C, Giner A, Ansorge W, Fotsis T *et al.* Dual function of rhoD in vesicular movement and cell motility. *Eur J Cell Biol* 2001; **80**: 391–398.
16 Tsubakimoto K, Matsumoto K, Abe H, Ishii J, Amano M, Kaibuchi K *et al.* Small GTPase RhoD suppresses cell migration and cytokinesis. *Oncogene* 1999; **18**: 2431–2440.
17 Gasman S, Kalaidzidis Y, Zerial M. RhoD regulates endosome dynamics through Diaphanous-related formin and Src tyrosine kinase. *Nat Cell Biol* 2003; **5**: 195–204.
18 Zanata SM, Hovatta I, Rohm B, Puschel AW.. Antagonistic effects of Rnd1 and RhoD GTPases regulate receptor activity in Semaphorin 3A-induced cytoskeletal collapse. *J Neurosci* 2002; **22**: 471–477.
19 Tong Y, Chugha P, Hota PK, Alviani RS, Li M, Tempel W *et al.* Binding of Rac1, Rnd1, and RhoD to a novel Rho GTPase interaction motif destabilizes dimerization of the plexin-B1 effector domain. *J Biol Chem* 2007; **282**: 37215–37224.
20 Moll R, Franke W, Schiller D, Geiger B, Krepler R. The catalogue of human cytokeratins: patterns of expression in nromal epithelia, tumors and cancer cells. *Cell* 1982; **31**: 11–24.
21 Stoler A, Kopan R, Duvic M, Fuchs E. Use of specific antibodies and cDNA probes to localize the major changes in keratin expression during normal and abnormal epidermal differentiation. *J Cell Biol* 1988; **107**: 427–446.
22 Rain JC, Selig L, De Reuse H, Battaglia V, Reverdy C, Simon S *et al.* The protein-protein interaction map of Helicobacter pylori. *Nature* 2001; **409**: 211–215.
23 Kato T, Watanabe N, Morishima Y, Fujita A, Ishizaki T, Narumiya S.. Localization of a mammalian homolog of diaphanous, mDia1, to the mitotic spindle in HeLa cells. *J Cell Sci* 2000; **114**: 775–784.
24 Kubo A, Tsukita S. Non-membranous granular organelle consisting of PCM-1: subcellular distribution and cell-cycle-dependent assembly/disassembly. *J Cell Sci* 2003; **116**(Part 5): 919–928.
25 Balczon R, Bao L, Zimmer WE, Brown K, Zinkowski RP, Brinkley BR. Dissociation of centrosome replication events from cycles of DNA synthesis and mitotic division in hydroxyurea-arrested Chinese hamster ovary cells. *J Cell Biol* 1995; **130**: 105–115.

26 Cizmecioglu O, Arnold M, Bahtz R, Settele F, Ehret L, Haselmann-Weiss U *et al.* Cep152 acts as a scaffold for recruitment of Plk4 and CPAP to the centrosome. *J Cell Biol* 2010; **191**: 731–739.
27 Warnke S, Kemmler S, Hames RS, Tsai HL, Hoffmann-Rohrer U, Fry AM *et al.* Polo-like kinase-2 is required for centriole duplication in mammalian cells. *Curr Biol* 2004; **14**: 1200–1207.
28 Ma Z, Kanai M, Kawamura K, Kaibuchi K, Ye K, Fukasawa K. Interaction between ROCK II and nucleophosmin/B23 in the regulation of centrosome duplication. *Mol Cell Biol* 2006; **26**: 9016–9034.
29 Hu W, Bellone CJ, Baldassare JJ. RhoA stimulates p27(Kip) degradation through its regulation of cyclin E/CDK2 activity. *J Biol Chem* 1999; **274**: 3396–3401.
30 Yamamoto M, Marui N, Sakai T, Morii N, Kozaki S, Ikai K *et al.* ADP-ribosylation of the rhoA gene product by botulinum C3 exoenzyme causes Swiss 3T3 cells to accumulate in the G1 phase of the cell cycle. *Oncogene* 1993; **8**: 1449–1455.
31 Olsen MF, Paterson HF, Marshall CJ. Signals from Ras and Rho GTPases interact to regulate the expression of p21 $^{waf1/cip1}$. *Nature* 1998; **394**: 295–299.
32 Villalonga P, Ridley AJ. Rho GTPases and cell cycle control. *Growth Factors* 2006; **24**: 159–164.
33 Carrano AC, Eytan E, Hershko A, Pagano M. SKP2 is required for ubiquitin-mediated degradation of the CDK inhibitor p27. *Nat Cell Biol* 1999; **1**: 193–199.
34 Lacey KR, Jackson PK, Stearns T. Cyclin-dependent kinase control of centrosome duplication. *Proc Natl Acad SciUSA* 1999; **96**: 2817–2822.
35 Hinchcliffe EH, Li C, Thompson EA, Maller JL, Sluder G. Requirement of Cdk2-cyclin E activity for repeated centrosome reproduction in Xenopus egg extracts. *Science (New York, NY)* 1999; **283**: 851–854.
36 Okuda M, Horn HF, Tarapore P, Tokuyama Y, Smulian AG, Chan PK *et al.* Nucleophosmin/B23 is a target of CDK2/cyclin E in centrosome duplication. *Cell* 2000; **103**: 127–140.
37 Tokuyama Y, Horn HF, Kawamura K, Tarapore P, Fukasawa K. Specific phosphorylation of nucleophosmin on Thr(199) by cyclin-dependent kinase 2-cyclin E and its role in centrosome duplication. *J Biol Chem* 2001; **276**: 21529–21537.
38 Cizmecioglu O, Warnke S, Arnold M, Duensing S, Hoffmann I. Plk2 regulated centriole duplication is dependent on its localization to the centrioles and a functional polo-box domain. *Cell Cycle* 2008; **7**: 3548–3555.
39 Krause A, Hoffmann I. Polo-like kinase 2-dependent phosphorylation of NPM/B23 on serine 4 triggers centriole duplication. *PLoS One* 2010; **5**: e9849.
40 Habedanck R, Stierhof YD, Wilkinson CJ, Nigg EA. The Polo kinase Plk4 functions in centriole duplication. *Nat Cell Biol* 2005; **7**: 1140–1146.
41 Kleylein-Sohn J, Westendorf J, Le Clech M, Habedanck R, Stierhof YD, Nigg EA. Plk4-induced centriole biogenesis in human cells. *Dev Cell* 2007; **13**: 190–202.
42 Eckerdt F, Yamamoto TM, Lewellyn AL, Maller JL. Identification of a polo-like kinase 4-dependent pathway for *de novo* centriole formation. *Curr Biol* 2011; **21**: 428–432.
43 Panopoulou E, Gillooly DJ, Wrana JL, Zerial M, Stenmark H, Murphy C *et al.* Early endosomal regulation of Smad-dependent signaling in endothelial cells. *J Biol Chem* 2002; **277**: 18046–18052.
44 Bellou S, Hink MA, Bagli E, Panopoulou E, Bastiaens PI, Murphy C *et al.* VEGF autoregulates its proliferative and migratory ERK1/2 and p38 cascades by enhancing the expression of DUSP1 and DUSP5 phosphatases in endothelial cells. *Am J Physiol Cell Physiol* 2009; **297**: C1477–C1489.
45 Panopoulou E, Murphy C, Rasmussen H, Bagli E, Rofstad EK, Fotsis T. Activin A suppresses neuroblastoma xenograft tumor growth via antimitotic and anti-angiogenic mechanisms. *Cancer Res* 2005; **65**: 1877–1886.
46 Sflomos G, Kostaras E, Panopoulou E, Pappas N, Kyrkou A, Politou AS *et al.* ERBIN is a new SARA-interacting protein: competition between SARA and SMAD2 and SMAD3 for binding to ERBIN. *J Cell Sci* 2011; **124**: 3209–3222.
47 Christoforidis S, Zerial M. Purification and identification of novel Rab effectors using affinity chromatography. *Methods* 2000; **20**: 403–410.

Supplementary Information accompanies the paper on the Oncogene website (http://www.nature.com/onc)